

Physiological mechanism of the overproduction of ϵ -poly-L-lysine by acidic pH shock in fed-batch fermentation

Xi-Dong Ren¹ · Xu-Sheng Chen¹ · Lei Tang¹ · Xin Zeng¹ · Liang Wang¹ · Zhong-Gui Mao¹

Received: 14 May 2015 / Accepted: 22 July 2015 / Published online: 11 August 2015
© Springer-Verlag Berlin Heidelberg 2015

Abstract The introduction of an environmental stress of acidic pH shock had successfully solved the common deficiency existed in ϵ -PL production, viz. the distinct decline of ϵ -PL productivity in the feeding phase of the fed-batch fermentation. To unravel the underlying mechanism, we comparatively studied the physiological changes of *Streptomyces* sp. M-Z18 during fed-batch fermentations with the pH shock strategy (PS) and pH non-shock strategy (PNS). Morphology investigation showed that pellet-shape change was negligible throughout both fermentations. In addition, the distribution of pellet size rarely changed in the PS, whereas pellet size and number decreased substantially with time in the PNS. This was consistent with the performances of ϵ -PL productivity in both strategies, demonstrating that morphology could be used as a predictor of ϵ -PL productivity during fed-batch fermentation. Furthermore, a second growth phase happened in the PS after pH shock, followed by the re-appearance of live mycelia in the dead core of the pellets. Meanwhile, mycelia respiration and key enzymes in the central metabolic and ϵ -PL biosynthetic pathways were overall strengthened until the end of the fed-batch fermentation. As a result, the physiological changes induced by the acidic pH shock have

synergistically and permanently contributed to the stimulation of ϵ -PL productivity. However, this second growth phase and re-appearance of live mycelia were absent in the PNS. These results indicated that the introduction of a short-term suppression on mycelia physiological metabolism would guarantee the long-term high ϵ -PL productivity.

Keywords ϵ -Poly-L-lysine · Acidic pH shock · Morphology · Key enzymes

Introduction

As a homopolymer of amino acid, ϵ -poly-L-lysine (ϵ -PL), consisting of 25–35 L-lysine residues, is linked by the isopeptide bond between α -carboxyl and ϵ -amino groups [1]. Owing to its unique property, ϵ -PL has been widely used as a natural food preservative in Japan, South Korea, the United States, and China [2, 3]. Moreover, ϵ -PL and its derivatives have also obtained wide spread application in the fields of food, medicine, environment, and electronics [4]. Nowadays, the role of ϵ -PL is becoming increasingly important.

To date, ϵ -PL production is mainly based on microbial fed-batch fermentation by *Streptomyces*. Fermentation process regulation, including pH control, immobilized cells, in situ product removal, and addition of citric acid and oxygen-vectors, has played an important role in the enhancement of ϵ -PL production [5–10]. These studies have mainly focused on the optimization of ϵ -PL productivity in shake flask and/or batch fermentations, whereas the performance of ϵ -PL productivity in the feeding phase of the fed-batch fermentation was scarcely concerned. In fact, the feeding phase usually occupied about 70 % of the whole fed-batch fermentation period, thereby the

Electronic supplementary material The online version of this article (doi:10.1007/s00449-015-1448-x) contains supplementary material, which is available to authorized users.

✉ Xu-Sheng Chen
chenxs@jiangnan.edu.cn

✉ Zhong-Gui Mao
maozg@jiangnan.edu.cn

¹ The Key Laboratory of Industrial Biotechnology, Ministry of Education, School of Biotechnology, Jiangnan University, 1800 Lihu Road, Wuxi 214122, Jiangsu, China

performance of ϵ -PL productivity in this phase was critical. However, the conspicuous decline of ϵ -PL productivity in the feeding phase of the fed-batch fermentation was almost inevitable. To exemplify, ϵ -PL productivity decreased distinctly at about 90 h in the fed-batch fermentation of *Kitasatospora* sp. MY 5–36 with both free and immobilized cells [7]. The similar results were also discovered in fed-batch fermentations for ϵ -PL production by *Streptomyces* [8–10]. Moreover, Jia et al. found that the accumulation of ϵ -PL production almost stopped after 96 h even carbon source was continually consumed [11]. This deficiency would be against the extension of fermentation period and the increase of final ϵ -PL production.

Until recently, we have firstly employed an environmental stress of acidic pH shock to enhance ϵ -PL production [3]. After the systematic optimization of batch fermentation parameters, fed-batch fermentation with glycerol and $(\text{NH}_4)_2\text{SO}_4$ feeding was conducted to explore the sufficient ϵ -PL production. Finally, ϵ -PL production in the pH shock strategy (designated as PS) reached 54.70 g/L at 8 days, which was 52.50 % higher than that of the pH non-shock strategy (designated as PNS). This is also the highest ϵ -PL production reported in literature so far. Notably, ϵ -PL productivity in the PS increased after the acidic pH shock and stabilized relatively until the end of the fed-batch fermentation. In contrast, ϵ -PL productivity in the PNS decreased distinctly in the feeding phase of the fed-batch fermentation as well as the previous studies [7–11]. Therefore, both fermentation strategies have provided excellent models to study the common issue existed in the fed-batch fermentation for ϵ -PL production.

In this study, we comparatively studied the physiological changes of mycelia during fed-batch fermentations for ϵ -PL production in the PS and the PNS, including the differences in morphology, viability, respiratory activity, and key enzymes in the central metabolic and ϵ -PL biosynthetic pathways. The investigation would help disclose the underlying mechanism involved in the superiority that caused by the acidic pH shock. To the best of our knowledge, this is the first study on the investigation of mycelia physiological changes during the fed-batch fermentation for ϵ -PL production.

Materials and methods

Microorganism, culture media and inoculum preparation

The strain *Streptomyces* sp. M-Z18 was used throughout this study, which was a mutagenesis from *Streptomyces albulus* Z-18 (CGMCC 10479) [3]. Agar slant medium, used to maintain the strain, composed of (g/L) glucose, 10;

yeast extract, 5; beef extract, 5; $\text{MgSO}_4 \cdot 7\text{H}_2\text{O}$, 0.5; $\text{K}_2\text{HPO}_4 \cdot 3\text{H}_2\text{O}$, 1; and agar, 20, along with pH 7.0 before sterilization [6]. Seed culture medium (M3G) contained (g/L) glucose, 50; yeast extract, 5; $(\text{NH}_4)_2\text{SO}_4$, 10; KH_2PO_4 , 1.36; $\text{K}_2\text{HPO}_4 \cdot 3\text{H}_2\text{O}$, 0.8; $\text{MgSO}_4 \cdot 7\text{H}_2\text{O}$, 0.5; $\text{ZnSO}_4 \cdot 7\text{H}_2\text{O}$, 0.04; and $\text{FeSO}_4 \cdot 7\text{H}_2\text{O}$, 0.03 [5]. The fermentation medium employing agro-industrial by-products consisted of (g/L) industrial glycerol, 83; $(\text{NH}_4)_2\text{SO}_4$, 8; fish meal, 15; corn steep liquor, 5; KH_2PO_4 , 5; $\text{MgSO}_4 \cdot 7\text{H}_2\text{O}$, 2; and $\text{FeSO}_4 \cdot 7\text{H}_2\text{O}$ 0.1 [12]. Initial pH values of the above two media were adjusted to 6.8 with 2 M NaOH and/or 1 M H_2SO_4 . All the media were sterilized in an autoclave for 20 min at 121 °C. In each case, glucose was autoclaved separately. The slants were inoculated and incubated at 30 °C for 7 days to obtain a heavy sporulated growth. After that time, spores were used for seed culture inoculation (in a concentration of about 2×10^5 spores/mL). The seed culture was grown in a 500-mL shake flask containing 80 mL of liquid medium and incubated at 30 °C on a rotary shaker (200 rpm) for 24 h.

Bioreactor cultures

A 5-L fermenter (BIOTECH-5BG, BaoXing Bio-Engineering Equipment Co., Ltd., Shanghai, China) with a 3.5-L working volume and two Rushton turbines was employed for fed-batch fermentation in this study. Before the inoculation, temperature, aeration rate, and agitation speed were maintained at 30 °C, 0.5 vvm and 200 rpm, respectively, and initial pH was controlled at 6.8 via manual addition of ammonia water (12.5 %, w/v). Approximately 300 mL of seed culture was used as the inoculum. Dissolved oxygen (DO) was set above 30 % of air saturation before pH declined to 4.0 and above 20 % of air saturation afterwards, which was controlled by manually adjusting agitation speed by the step of 50 rpm from 200 to 800 rpm during fermentation course. When agitation speed reached 800 rpm, aeration rate was then manually increased by the step of 0.5 vvm with a range of 0.5–2.5 vvm. During the fermentation process, pH and DO were, respectively, monitored online by pH and DO electrodes (K8S-225 and InPro6800, Mettler Toledo, Greifensee, Switzerland), while dry cell weights (DCW), ϵ -PL production, glycerol, and NH_4^+ -N were analyzed offline as described in the section of “Analytical methods.” Fed-batch fermentation started when the concentration of glycerol in the fermentation broth was below 10 g/L, and then sterilized pure glycerol was automatically added by peristaltic pump to maintain it at about 10 g/L. Residual ammonia nitrogen (NH_4^+ -N) was maintained at about 0.5 g/L by feeding 600 g/L sterilized $(\text{NH}_4)_2\text{SO}_4$ solution just as the feeding of glycerol.

Image analysis

The drawn samples were directly diluted with saline (0.9 % NaCl) to about 10^5 – 10^6 pellets/mL. Then, twenty microliter samples were deposited on a clean slider and covered with a cover slip. Images of mycelia were captured by a CCD camera (Leica DFC 450) mounted on a microscope (Leica DM 1000). Morphological measurements were carried out using the Leica Application Suite V4 software (all from Leica Microsystems, Wetzlar, Germany). Measurements of mycelia morphology were done on images obtained using 4× objective. Distributions were generated with a population size of approximately 150 pellets per sample.

CTC staining

5-cyano-2,3-ditolyl-tetrazolium chloride (CTC) is a soluble and non-fluorescing stain. It could be adsorbed and reduced into an insoluble red-fluorescent substance (CTC formazan) by respiring cells via the electron transport chain and accumulate in the cell. Therefore, this redox dye has been widely used to determine the respiratory activity of bacteria [13]. The higher fluorescence intensity represents higher respiratory activity. Biomass samples drawn at different time points from the bioreactor were centrifuged, washed twice, and re-suspended with saline (0.9 % NaCl) to about 10^5 – 10^6 pellets/mL. CTC staining was conducted in a 1.5-mL Eppendorf tube by use of a Bacstain-CTC rapid staining kit (Dojindo Laboratories, Kumamoto, Japan) for 30 min at 30 °C according to the manufacturer's instructions. Twenty microliter of stained samples were deposited on a clean slider and observed under a Leica confocal laser-scanning microscope (TCS-SP8, Leica Microsystems, Wetzlar, Germany) at the excitation wavelength of 488 nm and emission wavelength from 620 to 640 nm. Fluorescence intensity was quantified with the software provided by the manufacturer. A significant number of images were analyzed in a minimum of three independent culture analyses.

Viability staining

To evaluate the viability of the cultured mycelia, the LIVE/DEAD Bac-Light Bacterial Viability Kit L-13152 (Invitrogen detection technologies, California, USA) containing two nucleic acid staining dyes, propidium iodide (PI), and SYTO 9 was used. The SYTO9 is a green fluorescent stain which enters all the cells, those with intact membranes as well as those with damaged ones. In contrast, PI only penetrates dead cells with damaged membranes. However, PI has a higher affinity for the nucleic acids and displaces SYTO 9 in dead cells. Therefore, in the presence of both

stains, bacteria with intact cell membranes appear to be fluorescent green, whereas bacteria with damaged membranes appear red [14]. Culture samples were obtained and processed for microscopy at different time points, as previously described in section of “CTC staining.” The two stains were prepared and mixed together (1:1, v/v) as recommended by the manufacturer. Equal volume (20 μ L) of the stain mixture and culture samples were mixed on a clean slide and left in the dark for at least 10 min [15]. Then, the sample covered with a cover slip, analyzed under a Leica TCS-SP8 confocal laser-scanning microscope, was sequentially excited at wavelengths of 488 and 568 nm and observed at emission wavelengths of 530 nm (green) and 630 nm (red), respectively. A significant number of images were analyzed in a minimum of three independent culture analyses.

Average specific cell growth rate ($\bar{\mu}_x$) and average specific ϵ -PL formation rate ($\bar{\mu}_p$)

The values of $\bar{\mu}_x$ and $\bar{\mu}_p$ were calculated according to the following equations:

$$\bar{\mu}_{x_2} = \frac{1}{\bar{x}_{t_2}} \frac{\Delta x}{\Delta t} = \frac{1}{\frac{1}{2}(x_{t_2} + x_{t_1})} \times \frac{x_{t_2} - x_{t_1}}{t_2 - t_1}, \quad (1)$$

$$\bar{\mu}_{p_2} = \frac{1}{\bar{x}_{t_2}} \frac{\Delta p}{\Delta t} = \frac{1}{\frac{1}{2}(x_{t_2} + x_{t_1})} \times \frac{p_{t_2} - p_{t_1}}{t_2 - t_1}, \quad (2)$$

where x is DCW, p is ϵ -PL concentration, and t is fermentation time.

Analytical methods

Dry cell weights (DCW) determination: Ten-milliliter aliquots of culture broth was subjected to centrifugation at $4500 \times g$ for 10 min, and then the precipitate was collected and washed twice with distilled water. The washed mycelia were filtered through a pre-weighed filter paper and dried at 105 °C to a constant weight prior to measuring the biomass of the culture. The centrifugal supernatant was used to determine the ϵ -PL concentration according to the procedure described by Itzhaki [16]. The concentration of glycerol was determined using an HPLC system (U-3000, Dionex, Sunnyvale, USA) with a refractive index detector (Shodex RI-101, Tokyo, Japan) and an ion exchange column (Aminex HPX-87H, 300×7.8 mm, Hercules, CA). The column was eluted with 5 mM H_2SO_4 at a temperature of 60 °C and a flow rate of 0.6 mL/min. NH_4^+ -N was analyzed by means of a colorimetric method using Nessler reagent [17]. The intracellular enzyme activities were determined as described by Zeng et al. [18]. To check the reproducibility, the experiments were carried out at least duplicate.

Results and discussion

Performances of ϵ -PL production and cell growth in the pH shock and pH non-shock fed-batch fermentations

To elaborate the kinetic differences between both fermentations, time profiles of pH change, ϵ -PL production, cell growth, average specific ϵ -PL production rate ($\overline{\mu}_p$), and average specific cell growth rate ($\overline{\mu}_x$) are systematically compared in Fig. 1. In the PS, mycelia were first cultured at pH 5.0 until DCW was doubled, namely pre-acid-shock adaption. Then, acidic pH shock was conducted at about pH 3.0 for 12 h (from about 1 to 1.5 days). Finally, pH was restored to 4.0 for the subsequent fermentation. Unlike the PS, cells in the PNS failed to be stressed at the fatal pH of 3.0 (Fig. 1a). In both strategies, ϵ -PL production started after 1 day and increased for the rest of the fermentations. Compared to the PNS, ϵ -PL production in the PS was lower before 3 days but became higher afterwards (Fig. 1b). Likewise, the behaviors of cell growth showed similar trends as ϵ -PL production (Fig. 1c). In the pH shock phase, ϵ -PL production and cell growth were suppressed, resulting in the lower $\overline{\mu}_p$ and $\overline{\mu}_x$ of the PS at 2 days, compared to the PNS. However, after the pH shock, both ϵ -PL productivity and cell growth rate of the PS increased to above those of the PNS, which also caused the elevated $\overline{\mu}_p$ and $\overline{\mu}_x$.

Particularly for the $\overline{\mu}_p$, the higher performance sustained until the end of the fed-batch fermentation (Fig. 1b–e). As a result, the final ϵ -PL production and biomass in the PS reached 54.70 and 76.35 g/L at 8 days, which were 52.50 and 19.26 % higher than those of the PNS, respectively (Fig. 1b, c). Notably, ϵ -PL productivity in the PS stabilized relatively after 2 days (from 9.77 to 7.27 g/L/day), whereas it decreased distinctly in the PNS after 4 days (from 6.84 to 2.03 g/L/day) (Fig. 1b). In conclusion, the acidic pH shock is superior for ϵ -PL production, which could not only improve ϵ -PL productivity but also stabilize it relatively afterwards. Therefore, investigation on the underlying mechanism involved in such significant superiority for ϵ -PL production would be extremely interesting. Actually, acidic pH shock has also been successfully employed for the enhancement of other secondary metabolite productions by *Streptomyces* [19, 20]. For example, kasugamycin productivity by *Streptomyces kasugaensis* was even increased by sevenfold after acidic pH shock of 24 h [19]. Kim et al. considered that the enhanced effect of acidic pH shock on actinorhodin production by *Streptomyces coelicolor* A3(2) has attributed to the positive regulation of physiological metabolism, by means of upregulation of related sigma factors and shock proteins, regulators activation, and upregulation of genes associated with actinorhodin production, secretion, and the major central metabolic pathways [20, 21].

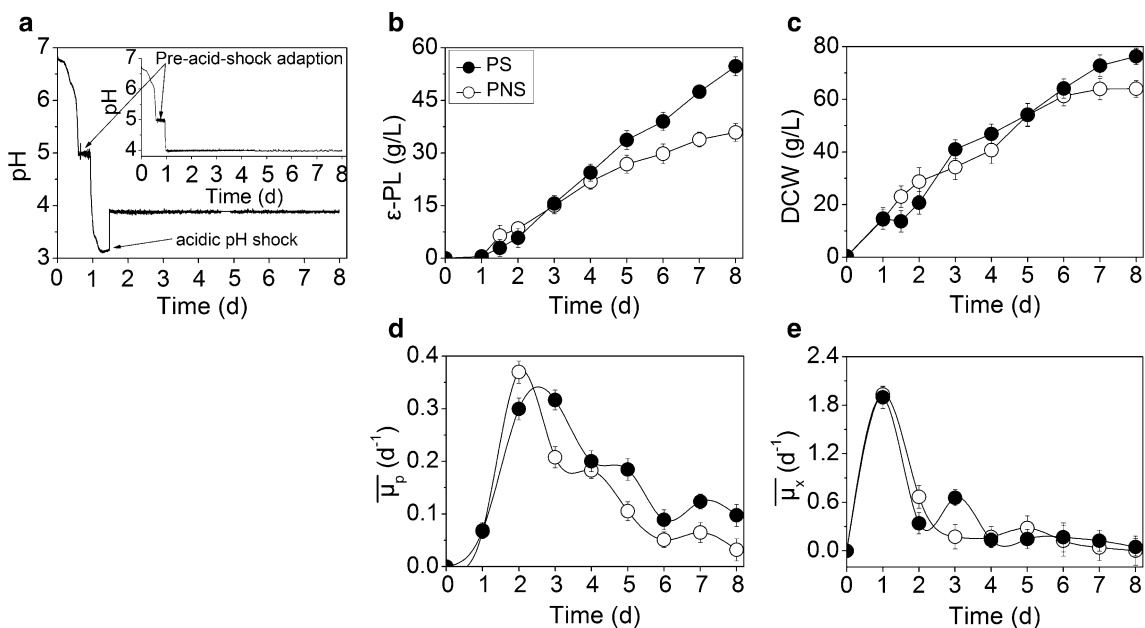


Fig. 1 Comparison of kinetic parameters between fed-batch fermentations for ϵ -PL production by *Streptomyces* sp. M-Z18 with the PS and the PNS. The micrograph in **a** indicates the time profile of pH

change in the fed-batch fermentation with the PNS. PS (filled circle); PNS (open circle)

Changes of mycelia morphology in the fed-batch fermentations for ϵ -PL production

Morphology is closely related to the production of secondary metabolites by *Streptomyces* [22]. Therefore, morphological changes of *Streptomyces* sp. M-Z18 including pellet size and shape during both fed-batch fermentations were the first consideration. The size of the pellet was estimated in terms of mean pellet diameter, while pellet shape was quantified as a ratio of the major to minor axis. At a first step towards the morphological changes, the changes of pellet size were compared between both strategies (Fig. 2a). In the PS, pellet size increased with cell growth after inoculation and reached the maximum of 220.3 μm at 1 day. Then, concomitant to the ceased cell growth, pellet disintegration happened in the pH shock phase, and the mean pellet diameter decreased to 168 μm at 2 days. After that, pellet size was stable for 2 days and then slowly increased to about 190 μm . It is noted that a second growth happened immediately after pH shock (Fig. 1c), whereas pellet size would not increase until cell growth to a certain extent after 4 days (Fig. 2a). In

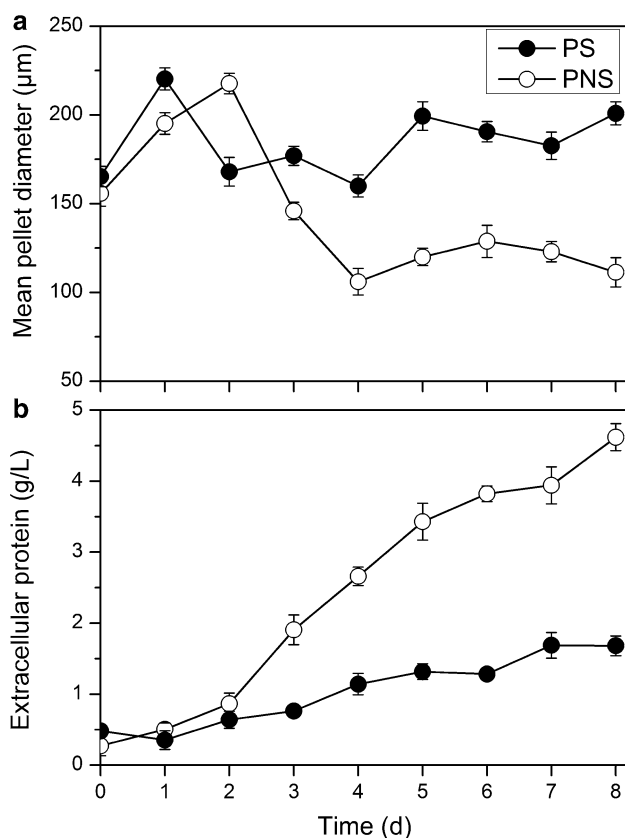


Fig. 2 Time profiles of pellet size and the accumulation of extracellular protein in fed-batch fermentations for ϵ -PL production by *Streptomyces* sp. M-Z18 with the PS and the PNS. PS (filled circle); PNS (open circle)

contrast, the size of pellets from the PNS kept increase until 2 days with the maximum value of 217.7 μm . Subsequently, sudden pellet disintegration occurred and pellet size rapidly decreased to about 110 μm at 4 days and stabilized to the end (Fig. 2a). Although pellet size was unchanged in the PNS after 4 days, pellet number was decreasing rapidly. As a result, mycelia existed in the pellet form could be rarely found in the PNS after 4 days, while pellet was the dominant form for the mycelia in the PS throughout the fed-batch fermentation (data not shown). Besides, the concentration of extracellular protein was used to indicate the extent of pellet disintegration (Fig. 2b). Compared to the PS, the accumulation of extracellular protein in the PNS was much faster after 2 days, which indicated that pellet disintegration in the PNS was more severe. This was in strong accordance with the rapid decrease of pellet size and number in the PNS after 2 days (Fig. 2a). Besides, the distribution of pellet size and shape during the fed-batch fermentations with both strategies was considered together (Fig. 3). It can be seen that there is no significant change in the distribution of pellet shape between both strategies throughout the fermentations. However, pellets with diameter above 200 μm disappeared in the PNS after 2 days (Fig. 3d–f), while the pellet size distribution in the PS was still polydisperse with plenty of pellets having size higher than 200 μm (Fig. 3a–c).

In conclusion, the distribution of pellet shape remained unchanged in both strategies. Besides, pellet size distribution in the PS was polydisperse and rarely changed throughout the fed-batch fermentation, whereas the severe pellet disintegration in the PNS resulted in the decreased pellet size and number. This was consistent with the performances of ϵ -PL productivity in both strategies. Therefore, morphology could be used as an indicator to monitor the performance of ϵ -PL productivity during fed-batch fermentation.

Changes of mycelia activity in the fed-batch fermentations for ϵ -PL production

In this section, mycelia activity including viability and respiratory activity was evaluated. Viability, i.e., the distribution of live and dead cells in pellets, was analyzed under confocal microscopy by means of viability staining with SYTO9 and propidium iodide (PI). Figure 4 shows the distribution of live and dead cells in the pellets from the PS and the PNS. At 0 day, the pellets of *Streptomyces* sp. M-Z18 in the PS were loose with appeared dead cells, moreover, an inner core of dead mycelia turned up in the larger pellets (Fig. 4a). The pellets became more compact at 1 day, and the inner core of dead cells grew up with time (Fig. 4b). At 2 days, the pellets became smooth and the peripheral mycelia were almost invisible. Besides, dead

Fig. 3 Distribution of pellet size and shape in fed-batch fermentations for ϵ -PL production by *Streptomyces* sp. M-Z18 with the PS and the PNS. PS (a–c); PNS (d–f)

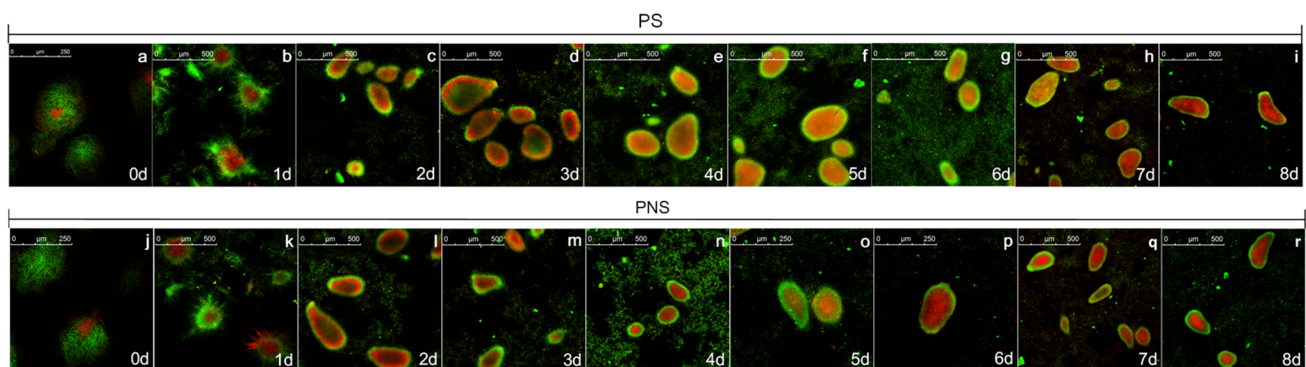
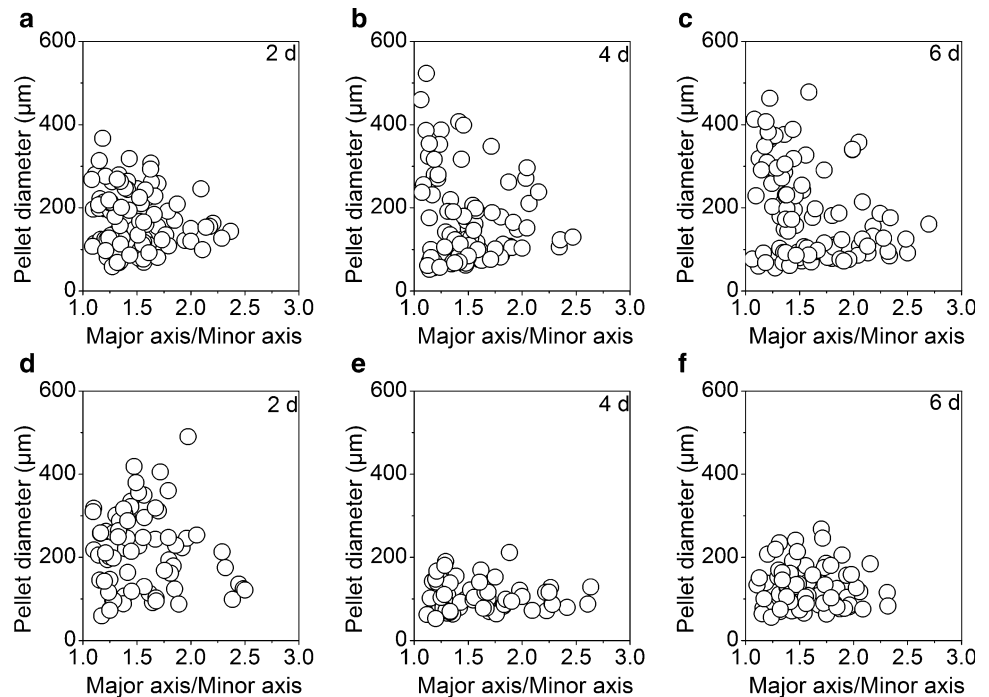


Fig. 4 Confocal laser-scanning microscopy of mycelia viability staining with SYTO9 and PI in fed-batch fermentations for ϵ -PL production by *Streptomyces* sp. M-Z18 with the PS and the PNS. Sample time point (days) and scale bar (micrometers) are indicated in each figure (a–r)

cells increased rapidly and consisted of the major fraction of pellets, whereas live cells were mainly found in the periphery of pellets. Meanwhile, dispersed live mycelia emerged around the pellets since 2 days, which may be attributed to the synergistic effect of the cell death and shear force (Fig. 4c). Notably, live mycelia appeared again in the dead core of pellets at 3 days (Fig. 4d). Then, cells inside the pellets resumed to death, and the interior of pellets were filled with dead cell mass from 4 days to the end of fermentation (Fig. 4e–i). However, the recovered live mycelia were absent in the pellets from the PNS, instead cells kept dying until the whole inner core of pellets were filled with dead cell mass (Fig. 4j–r). As is known, cell death from the center of pellets was a programmed process in the submerged culture of *Streptomyces*, which

was the prerequisite for the production of secondary metabolites [23]. In both strategies, cell death happened in the seed culture and proceeded since inoculation (Fig. 4). However, cell death was promoted by the acidic pH shock in the PS. While live cells could be easily found in the inner core of the pellets from the PNS at 2 days (Fig. 4l), the interior of the pellets from the PS was almost filled with dead cells (Fig. 4c). In the pH shock phase, mycelia were exposed to acid stress for 12 h, which would acidify the intracellular pH and cause damage to various macromolecules [24]. Eventually, cell death was promoted. Because of the promoted cell death, ϵ -PL production and cell growth were suppressed, resulting in the lower $\overline{\mu}_p$ and $\overline{\mu}_x$ of the PS at 2 days, compared to the PNS (Fig. 1). Notably, a second growth happened after the pH shock

(Fig. 1c), followed by the re-appearance of live mycelia in the dead center of the pellets from the PS at 3 days (Fig. 4d). Meanwhile, both $\bar{\mu}_p$ and $\bar{\mu}_x$ of the PS became to be higher than those of the PNS (Fig. 1d, e). It is deduced that the re-appearance of live mycelia was responsible for the elevated ε -PL productivity and cell growth rate. The re-appearance of live mycelia was also found in the pellets of *Amycolatopsis balhimycina*, but unlike *Streptomyces* sp. M-Z18 used in this study, it was not relevant to cell growth and product formation [15].

Respiratory activity of mycelia was determined by 5-cyano-2,3-ditotyl-tetrazolium chloride (CTC) staining. CTC formazan, which has a red fluorescence when excited by blue light, has accumulated inside all of the samples but with different fluorescence intensity (Supplementary Fig. S1). Moreover, the respiratory activity of mycelia was determined according to the fluorescence intensity of the CTC staining. As shown in Fig. 5, the respiratory activity of mycelia from both strategies decreased after inoculation, which attributed to the programmed cell death. Besides, compared to the PNS, the decreasing of mycelia respiratory activity in the PS was much faster after 1 day, with the respiratory activity of 64.69 % lower at 2 days. This difference was caused by the pH shock phase in which cell death was promoted (Fig. 4c). As expected, the respiratory activity of mycelia from the PS recovered along with the re-appearance of live mycelia, which gradually increased to 65.32 % of the control level at 4 days. Subsequently, mycelia respiratory activity in the PS decreased again to the final value of about 45.27 % of the control level. Conversely, the respiratory activity of mycelia from the PNS decreased continuously to the final value of about 34.46 % of the control level. As a result, mycelia

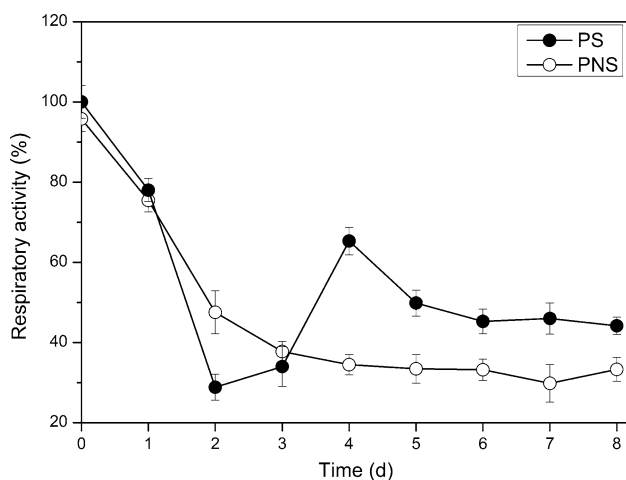


Fig. 5 Time profiles of respiratory activity in fed-batch fermentations for ε -PL production by *Streptomyces* sp. M-Z18 with the PS and the PNS. PS (filled circle); PNS (open circle)

respiratory activity in the PS was higher than that of the PNS after 3 days.

Therefore, in the pH shock phase, the promoted cell death resulted in the accelerated decrease of mycelia respiration. However, after pH shock, a second growth happened, followed by the re-appearance of live mycelia, which elevated mycelia respiratory activity of the PS to above the PNS until the end.

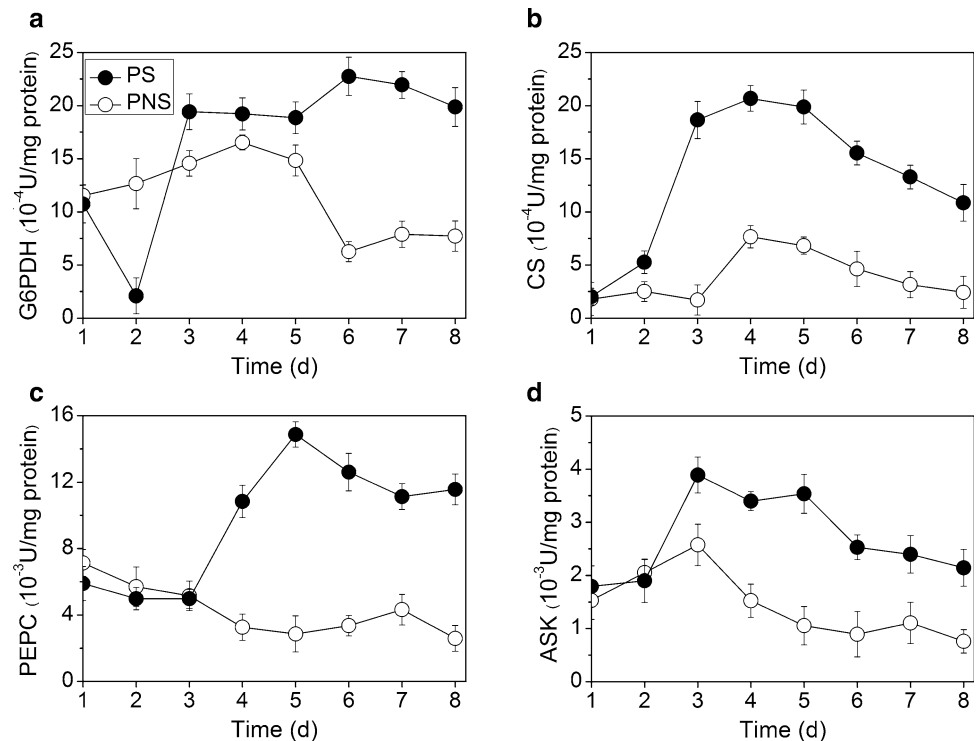
Changes of key enzymes in the fed-batch fermentations for ε -PL production

It is well known that enzymes are the fundament of physiological metabolism. In addition, the metabolic pathways with key enzymes of *Streptomyces* sp. M-Z18 for ε -PL production have already been elucidated in our previous study [18]. Therefore, the activities of four key enzymes in the central metabolic pathways corresponding to cell growth and ε -PL production, namely glucose-6-phosphate dehydrogenase (G6PDH) in the pentose phosphate pathway, citrate synthase (CS) in the TCA cycle, phosphoenolpyruvate carboxylase (PEPC) in the anaplerotic reaction, and aspartate kinase (ASK) in the ε -PL production pathway, were analyzed during both fed-batch fermentations, respectively (Fig. 6).

Pentose phosphate pathway could provide pentose and NADPH for cell growth and metabolite biosynthesis. It is seen that G6PDH activity of the PS was higher than that of the PNS since 3 days (Fig. 6a). This result was in agreement with the behaviors of cell growth in both strategies (Fig. 1c). In the pH shock phase, the promoted cell death resulted in lower G6PDH activity, which eventually ceased cell growth in the PS at 1.5 days. While after the pH shock, the re-appearance of live mycelia markedly increased the activity of G6PDH, cell growth was therefore enhanced. It is noted that the rapid decrease of G6PDH activity in the PNS happened after 5 days, which was in accordance with the strong inhibition of cell growth. However, G6PDH activity in the PS stabilized at a higher level since 3 days, which ensured the continuous cell growth in the feeding phase of the fed-batch fermentation (Fig. 1c). As is known, ε -PL production by *Streptomyces* sp. M-Z18 is in correlation with cell growth. Therefore, the stabilized G6PDH activity in the PS also contributed to the steady ε -PL productivity. Besides, NADPH is an essential cofactor for L-lysine synthesis [10]. The higher G6PDH activity in the PS could provide more NADPH for the enhancement of L-lysine production, which would be further polymerized to ε -PL by ε -PL synthetase.

The TCA circle is the major pathway that produces NADH and FADH₂. As shown in Fig. 6b, CS activity in the PS was much higher than that of the PNS after 2 days, which could provide more NADH and FADH₂. Moreover,

Fig. 6 Comparisons of key enzyme activities in the central metabolic and ϵ -PL biosynthetic pathways between fed-batch fermentations for ϵ -PL production by *Streptomyces* sp. M-Z18 with the PS and the PNS. PS (filled circle); PNS (open circle)



the respiratory activity of mycelia in the PS was higher than that of the PNS after 3 days, thereby more ATP would be generated via respiration in the PS. Yamanaka et al. had reported that ATP is essential for the function of ϵ -PL synthetase, and high levels of ATP are required for its sufficient catalytic activity [25, 26]. The enhancement of TCA circle could also provide more metabolic intermediates for the production of L-lysine, especially oxaloacetate (OAA). The anaplerotic reaction can replenish the consumed OAA, which directly converts phosphoenolpyruvate (PEP) into OAA. Figure 6c shows that PEPC activity in the PS increased to be much higher above the PNS after 3 days, indicating that more OAA was replenished for L-lysine synthesis. It is noted that the increase of PEPC activity was 1 day later than that of the CS activity in the PS, which may be the response of microorganism to the deficiency of the CS activity that caused by the enhanced L-lysine biosynthesis. The activity of ASK was also investigated to detect the change of the ϵ -PL production pathway. As shown in Fig. 6d, the ASK activity in the PS was higher than that of the PNS after 2 days. This improvement would supply more L-lysine for the production of ϵ -PL. Concomitant to the increased ATP production, ϵ -PL production would be further enhanced in the PS.

Therefore, the acidic pH shock markedly induced the redistribution of mycelia metabolism, while more metabolic flux flowed to ϵ -PL biosynthesis and energy generation.

In our previous study, a two-stage pH control strategy was developed based on the kinetic analysis of specific ϵ -PL formation rate in which pH was first controlled at 3.5 and then elevated to 3.8 for the subsequent fermentation [6]. After 173 h of fed-batch fermentation, ϵ -PL production reached 30.11 g/L, which was 41.89 % higher than that of the control strategy with single pH control of 3.8. Notably, ϵ -PL productivity in the two-stage pH control strategy stabilized relatively throughout the fed-batch fermentation, whereas ϵ -PL productivity in the single pH control strategy markedly decreased in the feeding phase of the fed-batch fermentation. These results were quite consistent with the phenomena observed in the fed-batch fermentations with the PS and the PNS in this study. In fact, pH 3.5 was also a stress for *Streptomyces* sp. M-Z18, even though the suppression effect was slighter than that of the pH 3.0. Compared to pH 3.8, both cell growth and glycerol consumption were slower at pH 3.5 [6]. Moreover, the respiratory activity of mycelia was also suppressed at pH 3.5, indicated by the increasing dissolve oxygen concentration (unpublished data). Besides, the suppression effect of pH 3.5 was more severe in ϵ -PL production by *Streptomyces albulus* IFO 14147 in which cell lysis and ceased glucose consumption happened [27]. Therefore, we could deduce that the short-term suppression on mycelia physiological metabolism by lower pH would guarantee the long-term higher ϵ -PL productivity. Furthermore, the suppression of mycelia physiological metabolism by other environmental

factors, e.g., nutrition and temperature, may be also benefit for ϵ -PL production.

Conclusion

Based on these combined observation, the acidic pH shock had influenced the physiological metabolism of the *Streptomyces* sp. M-Z18 in a concerted manner. In the pH shock phase, the promoted cell death was responsible for the suppressed ϵ -PL productivity and cell growth. After the acidic pH shock, a second growth happened, followed by the re-appearance of the live mycelia in the dead core of pellets, which improved mycelia respiratory activity. Meanwhile, the activities of key enzymes in the central metabolic and ϵ -PL biosynthetic pathways were overall markedly enhanced. As a result, both carbon metabolism and energy metabolism were strengthened after pH shock and maintained at higher level until the end. Based on the above enhancement, ϵ -PL productivity was improved after pH shock and stabilized relatively afterwards. Besides, the acidic pH shock could also impact mycelia morphology. In the PS, the distribution of pellet size was rarely changed, while pellet size and number in the PNS decreased substantially with time. The information obtained would provide important information to further improve ϵ -PL production for the whole industry. Further investigation on the transcriptional changes induced by the acidic pH shock would provide important information for the direct manipulation of *Streptomyces* sp. M-Z18 metabolism by metabolic engineering.

Acknowledgments This work was financially supported by the National Natural Science Foundation of China (31301556, 21376106), the Jiangsu Key Project of Scientific and Technical Supporting Program (BE2012616), the Cooperation Project of Jiangsu Province among Industries, Universities and Institutes (BY2013015-11), the Jiangsu Province “Collaborative Innovation Center for Advanced Industrial Fermentation” Industry Development Program, the Priority Academic Program Development of Jiangsu Higher Education Institutions, and the 111 Project (111-2-06).

Compliance with ethical standards

Conflict of interest The authors declare that they have no conflict of interest.

References

- Shima S, Sakai H (1977) Polylysine produced by *Streptomyces*. *Agric Biol Chem* 41:1807–1809
- Shima S, Matsuoka H, Iwamoto T, Sakai H (1984) Antimicrobial action of ϵ -poly-L-lysine. *J Antibiot* 37:1449–1455
- Ren XD, Chen XS, Zeng X, Wang L, Tang L, Mao ZG (2015) Acidic pH shock induced overproduction of ϵ -poly-L-lysine in fed-batch fermentation by *Streptomyces* sp. M-Z18 from agro-industrial by-products. *Bioprocess Biosyst Eng* 38:1113–1125
- Shih IL, Shen MH, Van YT (2006) Microbial synthesis of poly(ϵ -lysine) and its various applications. *Bioresour Technol* 97:1148–1159
- Kahar P, Iwata T, Hiraki J, Park EY, Okabe M (2001) Enhancement of ϵ -polylysine production by *Streptomyces albulus* strain 410 using pH control. *J Biosci Bioeng* 91:190–194
- Chen XS, Li S, Liao LJ, Ren XD, Li F, Tang L, Zhang JH, Mao ZG (2011) Production of ϵ -poly-L-lysine using a novel two-stage pH control strategy by *Streptomyces* sp. M-Z18 from glycerol. *Bioprocess Biosyst Eng* 34:561–567
- Zhang Y, Feng X, Xu H, Yao Z, Ouyang P (2010) ϵ -Poly-L-lysine production by immobilized cells of *Kitasatospora* sp. MY 5-36 in repeated fed-batch cultures. *Bioresour Technol* 101:5523–5527
- Liu S, Wu Q, Zhang J, Mo S (2011) Production of ϵ -poly-L-lysine by *Streptomyces* sp. using resin-based, in situ product removal. *Biotechnol Lett* 33:1581–1585
- Xia J, Xu Z, Xu H, Feng X, Bo F (2014) The regulatory effect of citric acid on the co-production of poly(ϵ -lysine) and poly(L-diaminopropionic acid) in *Streptomyces albulus* PD-1. *Bioprocess Biosyst Eng* 37:2095–2103
- Xu Z, Bo F, Xia J, Sun Z, Li S, Feng X, Xu H (2015) Effects of oxygen-vectors on the synthesis of epsilon-poly-lysine and the metabolic characterization of *Streptomyces albulus* PD-1. *Biochem Eng J* 94:58–64
- Jia S, Wang G, Sun Y, Tan Z (2009) Improvement of ϵ -poly-L-lysine production by *Streptomyces albulus* TUST2 employing a feeding strategy. Paper presented at the 3rd international conference on bioinformatics and biomedical engineering, Beijing, China, 11–13 June 2009
- Ren XD, Chen XS, Tang L, Sun QX, Zeng X, Mao ZG (2015) Efficient production of ϵ -poly-L-lysine from agro-industrial by-products by *Streptomyces* sp. M-Z18. *Ann Microbiol* 65:733–743
- Winding A, Binnerup SJ, Sørensen J (1994) Viability of indigenous soil bacteria assayed by respiratory activity and growth. *Appl Environ Microbiol* 60:2869–2875
- Rioseras B, López-García MT, Yagüe P, Sánchez J, Manteca Á (2014) Mycelium differentiation and development of *Streptomyces coelicolor* in lab-scale bioreactors: programmed cell death, differentiation, and lysis are closely linked to undecylprodigiosin and actinorhodin production. *Bioresour Technol* 151:191–198
- Singh KP, Mahendra AL, Jayaraj V, Wangikar PP, Jadhav S (2013) Distribution of live and dead cells in pellets of an actinomycete *Amycolatopsis balhimycina* and its correlation with balhimycin productivity. *J Ind Microbiol Biotechnol* 40:235–244
- Itzhaki R (1972) Colorimetric method for estimating polylysine and poly-arginine. *Anal Biochem* 50:569–574
- AOAC International (formerly the Association of Official Analytical Chemists) (1995) Official methods of analysis arlington. AOAC International, VA
- Zeng X, Chen XS, Ren XD, Liu QR, Wang L, Sun QX, Tang L, Mao ZG (2014) Insights into the role of glucose and glycerol as a mixed carbon source in the improvement of ϵ -poly-L-lysine productivity. *Appl Biochem Biotechnol* 173:2211–2224
- Kim CJ, Chang YK, Chun GT (2000) Enhancement of kasugamycin production by pH shock in batch cultures of *Streptomyces kasugaensis*. *Biotechnol Prog* 16:548–552
- Kim YJ, Song JY, Moon MH, Smith CP, Hong SK, Chang YK (2007) pH shock induces overexpression of regulatory and biosynthetic genes for actinorhodin production in *Streptomyces coelicolor* A3(2). *Appl Microbiol Biotechnol* 76:1119–1130
- Kim YJ, Moon MH, Song JY, Smith CP, Hong SK, Chang YK (2008) Acidic pH shock induces the expressions of a wide range of stress-response genes. *BMC Genom* 9:604

22. Singh KP, Wangikar PP, Jadhav S (2012) Correlation between pellet morphology and glycopeptide antibiotic balhimycin production by *Amycolatopsis balhimycina* DSM 5908. *J Ind Microbiol Biotechnol* 39:27–35
23. Manteca A, Alvarez R, Salazar N, Yagüe P, Sanchez J (2008) Mycelium differentiation and antibiotic production in submerged cultures of *Streptomyces coelicolor*. *Appl Environ Microbiol* 74:3877–3886
24. Park YK, Bearson B, Bang SH, Bang IS, Foster JW (1996) Internal pH crisis, lysine decarboxylase and the acid tolerance response of *Salmonella typhimurium*. *Mol Microbiol* 20:605–611
25. Yamanaka K, Maruyama C, Takagi H, Hamano Y (2008) ϵ -Poly-L-lysine dispersity is controlled by a highly unusual nonribosomal peptide synthetase. *Nat Chem Biol* 4:766–772
26. Yamanaka K, Kito N, Imokawa Y, Maruyama C, Utagawa T, Hamano Y (2010) Mechanism of ϵ -poly-L-lysine production and accumulation revealed by identification and analysis of an ϵ -poly-L-lysine-degrading enzyme. *Appl Environ Microbiol* 76:5669–5675
27. Shih IL, Shen MH (2006) Optimization of cell growth and poly(ϵ -lysine) production in batch and fed-batch cultures by *Streptomyces albulus* IFO 14147. *Process Biochem* 41:1644–1649